Exotic Higgs Decays: Measuring NMSSM $h_{1,2} \to a_1 a_1$ at the International Linear Collider

T. Liu[1] and C.T. Potter[2]

[1]Hong Kong University
[2]University of Oregon

July 24, 2013

Abstract

The NMSSM is motivated by the μ-term problem of the MSSM. We investigate a scenario in which the 125 GeV state recently discovered at the LHC is identified as the next lightest CP-even Higgs boson (h_2) while the lightest CP-even Higgs boson (h_1) has so far escaped detection at LEPII and the LHC in decays $h_1 \to 2a_1$, where the a_1 is the lightest CP-odd Higgs boson. We evaluate the precision obtainable at the ILC in measuring NMSSM $h_1 \to 2a_1$ in leptonic final states with simulated events generated by the Whizard event generator with full simulation of the SiD detector.

1 Introduction

The discovery of a Higgs-like resonance at the CMS [1] and ATLAS [2] *heralds the beginning* of a new era of Higgs physics. As is well known, the Higgs in the Standard Model (SM) suffers divergent quantum corrections to its mass, caused by the big hierarchy between the electroweak (EW) scale and the Planck scale. In most new physics scenarios addressing the gauge hierarchy problem, the Higgs mass stabilization mechanism manifests itself through Higgs couplings absent in the SM. Separately, the Higgs is one of the two SM fields that can have renormalizable couplings to SM singlet operators [3]. The Higgs therefore might be the main window into new physics and *systematic studies on the Higgs properties should be pursued*, e.g, coupling extractions, CP measurements, exotic decay searches.

Exotic Higgs decays are of particular interest - any signal would be an unambiguous signature for *physics beyond the SM (BSM)*. Due to the *small* SM Higgs decay width ($\Gamma \sim 4$ MeV for $m_h \sim 125$ GeV), a small coupling between the Higgs boson and some light particles may *yield* a large exotic Higgs decay branching fraction. The current experimental bounds on possible beyond the SM (BSM) decay channels of the Higgs are still weak, $\sim 60\%$ at the 2σ C.L. [4–8]. Because the LHC *lacks* sensitivity in measuring the Higgs-glue-glue coupling directly, it is very difficult to constrain the upper bound for Br($h \to$ exotic) below 10%, even with the full 300 fb^{-1} data of the LHC14 [9]. Therefore, exotic Higgs decays are a very effective tool to explore possible and exciting new physics couplings to the Higgs boson.

On the experimental side, the LHC is expected to be upgraded to its designed beam energy $13-14$TeV at the end of 2014, and to collect *much* more data. This provides *a great opportunity* for searching for exotic Higgs decays. Motivated by this, systematic studies are being pursued by theorists in various contexts CITE. However, though the LHC may play a significant role in exploring exotic Higgs decays, its sensitivity *is* weak in some cases. The first one is that

the SM-like Higgs decays into soft or collimated τ leptons or b quarks, with or without missing particles. Another possibility is that the Higgs decays to purely missing particles. To have sensitivity to such searches, it is typical that $\sim \mathcal{O}(100-1000)\text{fb}^{-1}$ LHC14 data is required, given $\text{Br}(h \to \text{exotic}) > 10\%$, e.g., see CITE. This is either because of the hadronic collider environment at the LHC or due to the lack of kinematic features in the final states. If the branching ratios of such exotic decays are below 10%, searching for them at the LHC14 may become inconsequential to the exploration of the related new physics.

On the other hand, *this case may* be where a Higgs factory like the International Linear Collider (ILC) is invaluable. One motivation for constructing such a machine is that it can precisely measure the Higgs couplings, including the Higgs-glue-glue and Higgs self couplings. As is well known, solving *the* hierarchy problem typically requires BSM physics to enter the effective theory at TeV scale. If this is true, the Higgs couplings in the SM are expected to have a deviation of $\mathcal{O}(1\%)$ level [9]. Unless significant improvement can be achieved for suppressing systematic uncertainties, it *is* very difficult for the LHC14 to reach such sensitivity. The ILC however can do much better. It is expected to be able to measure a deviation of $\mathcal{O}(1\%)$ level, assuming reasonable integrated luminosity [9]. The ILC therefore provides a great *opportunity* to probe TeV scale BSM physics, by measuring the Higgs couplings.

In this work, we show that exotic Higgs decays provide another case, justifying the value of a Higgs machine like the ILC. That is, even if the the decay branching ratio of the exotic Higgs decays is of $\mathcal{O}(1\%)$ level, the ILC still *has* great potential for discovering them directly. The ILC, therefore, is a machine not only for precise measurements, but also for discoveries. Though exotic Higgs decays can occur in many contexts, for the consideration of representativity, we will work in the Next-to-minimal-Supersymmetric-SM (NMSSM). The R- and PQ-symmetry limits in the NMSSM provides supersymmetric benchmark for various exotic Higgs decays. As an illustration, we consider a specific case in the R-symmetry limit of the NMSSM where $h_1, h_2 \to a_1 a_1$ are significant CITE. a_1 is the lightest CP-odd Higgs boson and serves as an R-axion. To design the minimal strategies that ensure optimal coverage of the full space of models, we perform a collider analysis, using the method of simplified models. Then we *compare* between the LHC and the ILC performances. The studies in the following can be generalized to many of the other possibilities, e.g., $a_1 \to b\bar{b}$. Though the technical details are different, the conclusion should be qualitatively similar. That is, the ILC can serve as a discovery machine for exotic Higgs decays which are challenging for the LHC14.

2 NMSSM Higgs Parameters

A review of the Higgs sector of the NMSSM can be found in [10]. Briefly, its superpotential and softly SUSY breaking terms are given by

$$\begin{aligned} \mathbf{W} &= \lambda \mathbf{S H_u H_d} + \frac{\kappa}{3}\mathbf{S}^3, \\ V_{soft} &= m_{H_d}^2 |H_d|^2 + m_{H_u}^2 |H_u|^2 + m_S^2 |S|^2 + (-\lambda A_\lambda H_u H_d S + \frac{1}{3} A_\kappa \kappa S^3 + h.c.). \end{aligned} \quad (1)$$

Here H_d, H_u and S denote the neutral Higgs fields in the $\mathbf{H_d}$, $\mathbf{H_u}$ and $\mathbf{S}$ supernultiplets, respectively. Once the singlet scalar S obtain a VEV $\langle S \rangle = v_S$, an effective μ parameter $\mu_{\text{eff}} = \lambda v_S$ can be generated. The NMSSM Higgs sector is determined by six free parameters at tree level: $\lambda, \kappa, A_\lambda, A_\kappa, \tan\beta$ and μ_{eff}. In addition to the Higgs spectrum of the MSSM, the NMSSM contains one extra CP-even h and one extra CP-odd scalar a. With subscripts denoting mass ordering, the NMSSM Higgs sector includes neutral CP-odd a_1, a_2, neutral CP-even h_1, h_2, h_3 and charged H^+, H^-.

In contrast to the A of the MSSM, a very light NMSSM a_1 is both natural and phenomenologically viable [11]. If $m_{a_1} < 2m_{h_1}$ then $h_1 \to a_1 a_1$ may proceed and is identified with a

Parameter	Value	Scalar	Mass [GeV]	Decay	BR [%]
λ	0.3	a_1	10.3	$h_1 \to 2a_1$	85.4
κ	0.1	h_1	91.6	$h_1 \to b\bar{b}$	11.9
A_κ	11.6	h_2	124.5	$h_1 \to \tau^+\tau^-$	1.2
m_A	465 GeV	a_2	465.2	$a_1 \to \tau^+\tau^-$	73.2
$\tan\beta$	3.1	h_3	469.2	$a_1 \to 2g + c\bar{c}$	22.3+3.1
μ_{eff}	165 GeV	$H^\pm$	465.7	$a_1 \to \mu^+\mu^-$	0.3

Table 1: NMSSM parameter choices with the Higgs scalar mass spectrum and dominant branching ratios.

scenarioin which $m_{h_1} \approx 100$ GeV minimizes fine tuning in electroweak symmetry breaking [12]. This scenario may explain the LEPII 2σ excess near $m_{b\bar{b}} \approx 98$ GeV in the $Zb\bar{b}$ channel by suppressing $h_1 \to b\bar{b}$ []. For $m_{a_1} > 2m_B$, $a_1 \to b\bar{b}$ dominates. Limits on $h_1 \to a_1a_1 \to b\bar{b}b\bar{b}$ from LEPII rule out $m_{h_1} < 110$ GeV for $m_{a_1} > 2m_B$ [13]. In this study we investigate the case with $2m_\tau < m_{a_1} < 2m_B$ and $m_{h_1} \approx 98$ GeV. The most constraining limits on this scenario are set by the ALEPH collaboration [14]. While neither ATLAS nor CMS has reported searches for for this scenario, the LHC sensitivity is studied in [15].

In this scenario h_{125}, the 125 GeV boson recently observed at the LHC is identified with the NMSSM h_2. While signal strengths in various decay channels reported from CMS and ATLAS are consistent with the SM signal strengths, they are also consistent with a large branching ratio to invisible (or undetected) final states. ATLAS reports $BR(h_{125} \to invisible) < 65\%$ is excluded with a 95% confidence level for the observed, and 84% with 95% CL for the expected [16]. Since neither CMS nor ATLAS report searches in the channel $h_{125} \to a_1a_1$, these decays may proceed with high branching ratio yet still go undetected. Therefore $h_2 \to a_1a_1$ is also of interest.

We seek NMSSM Higgs model parameters $\lambda, \kappa, A_\lambda, A_\kappa, \tan\beta$ and μ_{eff} which yield $m_{a_1} \approx 10$ GeV, $m_{h_1} \approx 98$ GeV and $m_{h_2} \approx 125$ GeV. Radiative corrections in the Higgs sector require a full specification in other sectors. Motivated by *natural* SUSY [17], we also seek gaugino masses and soft SUSY breaking terms which yield light neutralinos and supersymmetric top quarks which can still avoid current LHC limits. We use NMSSMTools 3.2.4 [18–20] to calculate the mass spectrum, widths and branching ratios. See Table 1 for the chosen parameters and resulting masses and branching ratios. The value of A_λ is determined by the parameter $m_A = \frac{\lambda v_s}{\sin 2\beta}(\sqrt{2}A_\lambda + \kappa v_s)$ where $v_s = \sqrt{2} < S >$.

This model contains all of the interesting phenomenology described in Section 1, namely $h_1 \to a_1a_1$ and $a_1 \to \tau^+\tau^-$ dominant with $m_{a_1} \approx 10$ GeV, $m_{h_1} \approx 98$ GeV and $m_{h_2} \approx 125$ GeV. NMSSMTools reports that the model predicts values for $b \to s\gamma$, $B_s \to \mu^+\mu^-$, $B \to \tau\nu$ and the anomalous magnetic moment Δa_μ within experimental constraints. Moreover the lightest chargino mass $m_{\chi_1^+}$ is just at the PDG limit and the dark matter relic density is near the lower allowed limit.

The supersymmetric top phenomenology in this model evades current LHC limits by including i) a very light $\tilde{t}_1$ which must decay via $\tilde{t}_1 \to b\chi_1^+$ where $m_{\chi_1^+}$ lies just above the W mass and the χ_1^+ shares nearly identical branching ratios with the W (*stealth* stop scenario) and ii) a heavier $\tilde{t}_2$ which decays in more than 8 distinct channels with branching ratio above 1%, none of which is higher than $BR(\tilde{t}_2 \to b\chi_1^+) \approx 31\%$. Two channels, with $BR(\tilde{t}_2 \to W\tilde{b}_2) \approx 12\%$ and $BR(\tilde{t}_2 \to Z\tilde{t}_1) \approx 20\%$ have no public results from either ATLAS or CMS.

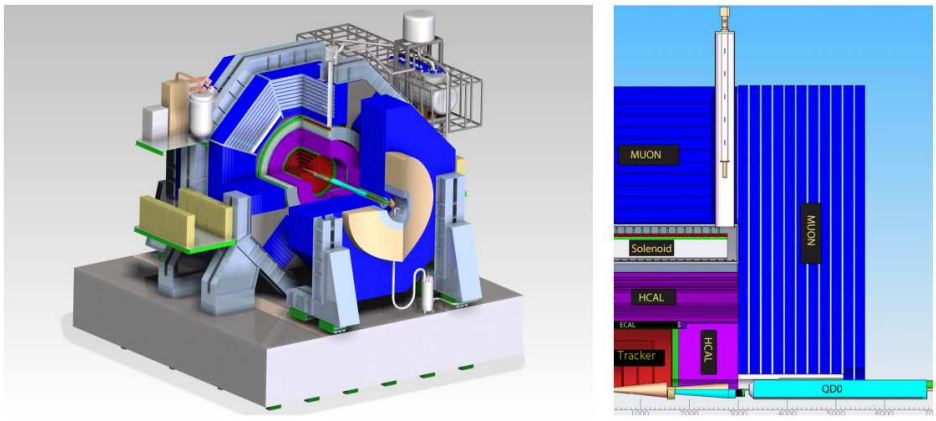

Figure 4.2. The SiD detector, showing (left) an isometric view on the platform, and (right) a quadrant section. Colour coding: tracking (red), ECAL (green), HCAL (violet) and the flux return (blue).

Figure 1: The SiD detector.

3 SiD Detector and Simulation

See Figure 1 for isometric and quadrant sections of the SiD detector. The SiD includes sub-detectors for charged particle tracking and vertex reconstruction near the interaction point, electromagnetic and hadronic calorimetery for charged and neutral particle calorimetry. The association of tracks in the tracker with clusters in the calorimetry is employed in a particle flow algorithm to improve the reconstruction of jets. Two calorimeters are placed in the forward region for luminosity measurement. Full details can be found in Volume 4 of the ILC Technical Design Report [21].

SiD comprises a compact vertex detector instrumented with silicon pixels for vertex reconstruction, a main tracker instrumented with silicon strips for measuring charged particle momentum, an electromagnetic calorimeter with silicon strips in the active layers and Tungsten in the passive layers for measuring electgromagnetic energy deposits, a hadronic calorimeter with glass resistive plate chambers in the active layers and steel in the passive layers for measuring hadronic energy deposits, and a muon system instrumented with scintillators in the iron flux return of a 5T solenoidal magnet.

The vertex detector extends radially in the region $1.4 < r < 6.0$cm and employs five layers around the beamline and five disks on both sides of the interaction point. The barrel and disks are instrumented with $20 \times 20\mu\text{m}^2$ pixels designed to timestamp each hit in order to reduce background between bunch crossings. The main tracker contains the vertex detector in the region $21.7 < r < 122.1$cm and consists of five cylinders and four disks on both sides of the interaction point, all instrumented with 10×10 cm^2 silicon sensors to achive a momentum resolution of $\delta(1/p_T) = 5 \times 10^{-5}\text{GeV}^{-1}$ and coverage down to a polar angle of 10°.

The electromagnetic calorimeter occupies the region $126.5 < r < 140.9$cm and includes 26 radiation lengths and one nuclear interaction length. In the active layers the $5 \times 5\text{mm}^2$ silicon sensors register energy depsosits. The hadronic calorimeter includes 4.5 nuclear interaction lengths and extends radially $141.7 < r < 249.3$cm.

Details of the event generation, detector simulation and event reconstruction can be found in [21]. After event generation, signal and background events are passed through a detector simulation with SLIC, a program with full GEANT4 [22] functionality. Energy deposits expected from generator particles are simulated in sensitive regions of the detector subsystems which are

Process	$\sqrt{s}$ [GeV]	Polarization [-%/+ %]	$\int dt\mathcal{L}$[fb^{-1}]
NMSSM Signal	250	-80/+30	250
NMSSM Signal	250	+80/-30	250
SM Background	250	-80/+30	250
SM Background	250	+80/-30	250
NMSSM Signal	350	-80/+30	350
NMSSM Signal	350	+80/-30	350
SM Background	350	-80/+30	350
SM Background	350	+80/-30	350
Top Pair	350	-80/+30	350
Top Pair	350	+80/-30	350

Table 2: The simulated data samples created from pure polarization samples with their equivalent luminosities. Each signal sample contains both h_1 and h_2 weighted by production cross section.

then digitized. Particles are then reconstructed as particle flow objects using particle flow algorithms.

The electron and positron beams at the ILC can be polarized in order to optimize measurements. The chosen polarizations for signal and background simulation samples are either 80% lefthanded e^- and 30% righthanded e^+, or 80% righthanded e^- and 30% lefthanded e^+. See Table 2 for the list of simulated data samples used in this analysis.

Simulation of the signal process $e^+e^- \to Zh_{1,2} \to f\bar{f}a_1a_1$ was performed with the Whizard event generator [23,24], which has a full implementation of the NMSSM [25]. Whizard interfaces the NMSSM model described in Section 2 with the SLHA [26] file generated by NMSSMTools.[1] Signal events are weighted by production cross section multiplied by the branching ratio for $Z \to f\bar{f}$. For a pure polarization state $e^-_L e^+_R$ ($e^-_R e^+_L$), the $\sqrt{s} = 250$ GeV cross section reported by Whizard for $Zh_1 \to \mu^+\mu^- a_1a_1$ is 17.034 ± 0.006 fb (13.105 ± 0.005 fb). For $Zh_2 \to \mu^+\mu^- a_1a_1$ it is 5.715 ± 0.002 fb (4.397 ± 0.002 fb). After weighting the event yields correspond to integrated luminosities of 250fb^{-1} (350fb^{-1}) for $\sqrt{s} = 250$ GeV ($\sqrt{s} = 350$ GeV).

Simulation of top pair and other SM backgrounds is also performed with Whizard. The dominant background to $h_{1,2} \to a_1a_1 \to 4\tau_{1-pr}$ is the process $e^+e^- \to ZZ \to \mu^+\mu^-\tau_{1-pr}\tau_{3-pr}$, so a high-statistics sample of this background is produced with Whizard.

4 Analysis of Simulated Data

The data analysis selection seeks to identify the dominant decays of the $h_{1,2}$ in the recoil of $Z \to \mu^+\mu^-$. Since the decay of τ to one-prongs (e, μ, π) is dominant we identify $h_{1,2} \to a_1a_1 \to 4\tau$ as four-track events in the recoil of the Z with net charge zero. The selection requirements are as follows:

- require at least two muons with $p_T > 5$ GeV ($N_{\mu 5} \geq 2$)
- require the muon pair closest to the Z mass within 3σ of the nominal Z mass ($|m_Z - m_{\mu^+\mu^-}| < 3\sigma$)
- require exactly four tracks with $p_T > 1$ GeV in the recoil ($N_{trk1} = 4$)
- require zero net charge in the recoil tracks ($Q_{4trk} = 0$)

[1] Thanks to Tim Barklow for generating the Whizard events and Norman Graf for detector simulation and event reconstruction

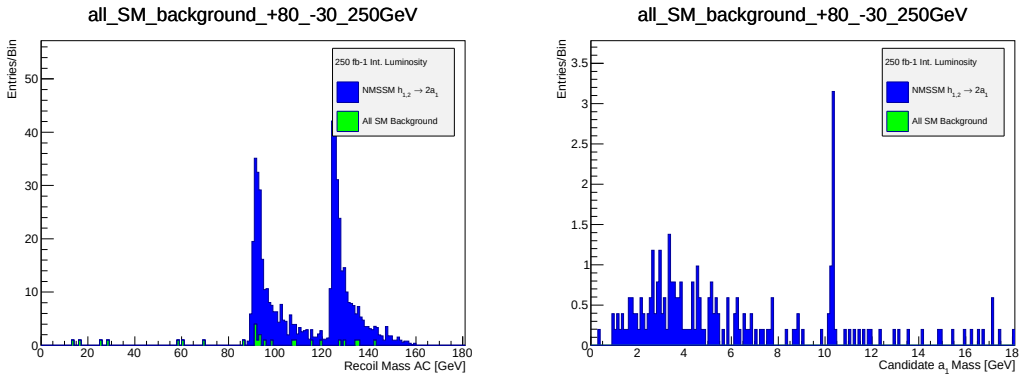

Figure 2: At left, the recoil masses after full analysis selection. At right, the reconstructed $a_1 \to \mu^+\mu^-$. The plots assume $\sqrt{s} = 250$ GeV with 250fb^{-1} integrated luminosity.

See Figure 2 (left) for the recoil mass distribution after full analysis selection.

After this selection we expect very little contamination from the hadronic decays $a_1 \to gg, c\bar{c}$ which form jets producing very high track multiplicity. On the other hand, this selection should be sensitive to $a_1 \to \mu^+\mu^-$. If we further require:

- require exactly two oppositely charged muons in the recoil ($N_{\mu 5} = 2$)

See Figure 2 (right) for the reconstructed $a_1 \to \mu^+\mu^-$ after full analysis selection..

5 Conclusion

Author's note: no conclusions are made in this draft.

References

[1] Serguei Chatrchyan et al. Observation of a new boson at a mass of 125 GeV with the CMS experiment at the LHC. *Phys.Lett.*, B716:30–61, 2012.

[2] Georges Aad et al. Observation of a new particle in the search for the Standard Model Higgs boson with the ATLAS detector at the LHC. *Phys.Lett.*, B716:1–29, 2012.

[3] Brian Patt and Frank Wilczek. Higgs-field portal into hidden sectors. 2006.

[4] G. Belanger, B. Dumont, U. Ellwanger, J.F. Gunion, and S. Kraml. Status of invisible Higgs decays. *Phys.Lett.*, B723:340–347, 2013.

[5] Pier Paolo Giardino, Kristjan Kannike, Isabella Masina, Martti Raidal, and Alessandro Strumia. The universal Higgs fit. 2013.

[6] Abdelhak Djouadi and Grgory Moreau. The couplings of the Higgs boson and its CP properties from fits of the signal strengths and their ratios at the 7+8 TeV LHC. 2013.

[7] Combined coupling measurements of the Higgs-like boson with the ATLAS detector using up to 25 fb^{-1} of proton-proton collision data. Technical Report ATLAS-CONF-2013-034, CERN, Geneva, Mar 2013.

[8] Combination of standard model Higgs boson searches and measurements of the properties of the new boson with a mass near 125 GeV. Technical Report CMS-PAS-HIG-13-005, CERN, Geneva, 2013.

[9] Michael E. Peskin. Comparison of LHC and ILC Capabilities for Higgs Boson Coupling Measurements. 2012.

[10] Ulrich Ellwanger, Cyril Hugonie, and Ana M. Teixeira. The Next-to-Minimal Supersymmetric Standard Model. *Phys.Rept.*, 496:1–77, 2010.

[11] Ulrich Ellwanger. Higgs Bosons in the Next-to-Minimal Supersymmetric Standard Model at the LHC. *Eur.Phys.J.*, C71:1782, 2011.

[12] Radovan Dermisek and John F. Gunion. The NMSSM Close to the R-symmetry Limit and Naturalness in $h \to aa$ Decays for $m_a < 2m_b$. *Phys.Rev.*, D75:075019, 2007.

[13] S. Schael et al. Search for neutral MSSM Higgs bosons at LEP. *Eur.Phys.J.*, C47:547–587, 2006.

[14] S. Schael et al. Search for neutral Higgs bosons decaying into four taus at LEP2. *JHEP*, 1005:049, 2010.

[15] David G. Cerdeno, Pradipta Ghosh, and Chan Beom Park. Probing the two light Higgs scenario in the NMSSM with a low-mass pseudoscalar. *JHEP*, 1306:031, 2013.

[16] Search for invisible decays of a higgs boson produced in association with a z boson in atlas. Technical Report ATLAS-CONF-2013-011, CERN, Geneva, Mar 2013.

[17] Michele Papucci, Joshua T. Ruderman, and Andreas Weiler. Natural SUSY Endures. *JHEP*, 1209:035, 2012.

[18] Ulrich Ellwanger, John F. Gunion, and Cyril Hugonie. NMHDECAY: A Fortran code for the Higgs masses, couplings and decay widths in the NMSSM. *JHEP*, 0502:066, 2005.

[19] Ulrich Ellwanger and Cyril Hugonie. NMHDECAY 2.0: An Updated program for sparticle masses, Higgs masses, couplings and decay widths in the NMSSM. *Comput.Phys.Commun.*, 175:290–303, 2006.

[20] G. Belanger, F. Boudjema, C. Hugonie, A. Pukhov, and A. Semenov. Relic density of dark matter in the NMSSM. *JCAP*, 0509:001, 2005.

[21] Chris Adolphsen, Maura Barone, Barry Barish, Karsten Buesser, et al. The international linear collider: Technical design report. volume 4: Detectors. Technical Report CERN-ATS-2013-037. ANL-HEP-TR-13-20. BNL-100603-2013-IR. IRFU-13-59. Cockcroft-13-10. CLNS-13-2085. DESY-13-062. FERMILAB-TM-2554. IHEP-AC-ILC-2013-001. ILC-REPORT-2013-040. INFN-13-04-LNF. JAI-2013-001. JINR-E9-2013-35. JLAB-R-2013-01. KEK-Report-2013-1. KNU-CHEP-ILC-2013-1. LLNL-TR-635539. SLAC-R-1004. ILC-HiGrade-Report-2013-003. arXiv:1306.6353, CERN, Geneva, Jun 2013.

[22] S. Agostinelli, J. Allison, K. Amako, J. Apostolakis, et al. Geant4 simulation toolkit. *Nuclear Instruments and Methods in Physics Research Section A: Accelerators, Spectrometers, Detectors and Associated Equipment*, 506(3):250 – 303, 2003.

[23] Wolfgang Kilian, Thorsten Ohl, and Jurgen Reuter. WHIZARD: Simulating Multi-Particle Processes at LHC and ILC. *Eur.Phys.J.*, C71:1742, 2011.

[24] Mauro Moretti, Thorsten Ohl, and Jurgen Reuter. O'Mega: An Optimizing matrix element generator. 2001.

[25] Jurgen Reuter and Felix Braam. The NMSSM implementation in WHIZARD. *AIP Conf.Proc.*, 1200:470–473, 2010.

[26] B.C. Allanach, C. Balazs, G. Belanger, M. Bernhardt, F. Boudjema, et al. SUSY Les Houches Accord 2. *Comput.Phys.Commun.*, 180:8–25, 2009.